THE JOURNAL OF BIOLOGICAL CHEMISTRY VOL. 288, NO. 1, pp. 223–233, January 4, 2013

Anticoagulant Activity of a Unique Sulfated Pyranosic (1→3)-β-L-Arabinan through Direct Interaction with Thrombin*[S]

Received for publication, May 29, 2012, and in revised form, October 19, 2012 Published, JBC Papers in Press, November 16, 2012, DOI 10.1074/jbc.M112.386441

Paula V. Fernández[‡], Irene Quintana[§], Alberto S. Cerezo[¶1], Julio J. Caramelo[‖1], Laercio Pol-Fachin[**], Hugo Verli[‡‡], José M. Estevez[§§1], and Marina Ciancia[‡¶1,2]**

From the [‡]Cátedra de Química de Biomoléculas, Departamento de Biología Aplicada y Alimentos, Facultad de Agronomía, Universidad de Buenos Aires, Av. San Martín 4453, 1417 Buenos Aires, Argentina, the [§]Laboratorio de Hemostasia y Trombosis, Departamento de Química Biológica, Facultad de Ciencias Exactas y Naturales, Universidad de Buenos Aires, Ciudad Universitaria, Pabellón 2, C1428EHA Buenos Aires, Argentina, the [¶]Centro de Investigaciones en Hidratos de Carbono (CIHIDECAR)-Consejo Nacional de Investigaciones Científicas y Técnicas (CONICET), Departamento de Química Orgánica, Facultad de Ciencias Exactas y Naturales, Universidad de Buenos Aires, Ciudad Universitaria, Pabellón 2, C1428EHA Buenos Aires, Argentina, the [‖]Instituto de Investigaciones Bioquímicas de Buenos Aires (IIBBA), CONICET, Av. Patricias Argentinas 435, 1405 Buenos Aires, Argentina, the [**]Programa de Pos-Graduação em Biologia Celular e Molecular, Centro de Biotecnologia, Universidade Federal do Rio Grande do Sul, Porto Alegre, Rio Grande do Sul, Brasil, the [‡‡]Faculdade de Farmácia, Universidade Federal do Rio Grande do Sul, 90610–000 Porto Alegre, Rio Grande do Sul, Brasil, and the [§§]Instituto de Fisiología, Biología Molecular y Neurociencias (IFIByNE-CONICET), Facultad de Ciencias Exactas y Naturales, Universidad de Buenos Aires, Ciudad Universitaria, Pabellón 2, C1428EHA Buenos Aires, Argentina

Background: Many seaweed polysaccharides have anticoagulant activity, but the mechanism of action was elucidated in a few cases.
Results: A highly sulfated pyranosic β-arabinan exerts its activity through direct and indirect inhibition of thrombin.
Conclusion: The structure and mechanism of action of the arabinan are different from those found for other polysaccharides.
Significance: This arabinan could be an alternative anticoagulant in certain specific cases.

A highly sulfated 3-linked β-arabinan (Ab1) with arabinose in the pyranose form was obtained from green seaweed *Codium vermilara* (Bryopsidales). It comprised major amounts of units sulfated on C-2 and C-4 and constitutes the first polysaccharide of this type isolated in the pure form and fully characterized. Ab1 showed anticoagulant activity by global coagulation tests. Less sulfated arabinans obtained from the same seaweed have less or no activity. Ab1 exerts its activity through direct and indirect (antithrombin- and heparin cofactor II-mediated) inhibition of thrombin. Direct thrombin inhibition was studied in detail. By native PAGE, it was possible to detect formation of a complex between Ab1 and human thrombin (HT). Ab1 binding to HT was measured by fluorescence spectroscopy. CD spectra of the Ab1 complex suggested that ligand binding induced a small conformational change on HT. Ab1-thrombin interactions were studied by molecular dynamic simulations using the persulfated octasaccharide as model compound. Most carbohydrate-protein contacts would occur by interaction of sulfate groups with basic amino acid residues on the surface of the enzyme, more than 60% of them being performed by the exosite 2-composing residues. In these interactions, the sulfate groups on C-2 were shown to interact more intensely with the thrombin structure. In contrast, the disulfated oligosaccharide does not promote major conformational modifications at the catalytic site when complexed to exosite 1. These results show that this novel pyranosic sulfated arabinan Ab1 exerts its anticoagulant activity by a mechanism different from those found previously for other sulfated polysaccharides and glycosaminoglycans.

Codium species biosynthesize a complex system of sulfated polysaccharides. Love and Percival (1) reported that the water-soluble polysaccharides from *Codium fragile* were composed, at least in part, of 3-linked galactopyranose and 3-linked arabinopyranose units, the former being sulfated on C-4 or C-6, whereas the arabinose residues were suggested to carry sulfate on either C-2 or C-4. Later, it was found that the room temperature water extracts of *C. fragile* and *Codium vermilara* were constituted by a family of sulfated polysaccharides comprising galactose and arabinose as major components (2, 3). Results obtained until now did not allow investigators to establish beyond doubt whether they are arabinogalactans or a mixture of arabinans and galactans. A lot of information has been obtained in recent years about the galactan structures, which were isolated in some cases in a pure form (2–6) with some small variations on the structures for different species; however, information about the arabinan moiety is scarce (2, 3, 7, 8).

Many different sulfated polysaccharides from seaweeds were found to have anticoagulant activity. The important differences

* This work was supported by grants from the National Research Council of Argentina, Consejo Nacional de Investigaciones Científicas y Técnicas (CONICET) Grant PIP 559/2010, and Agencia Nacional de Promoción Científica y Tecnológica (ANPCYT) Grant PICT 2008-0500 (to M. C.) and Conselho Nacional de Desenvolvimento Científico e Tecnológico (CNPq), Fundação de Amparo a Pesquisa do Estado do Rio Grande do Sul (FAPERGS), and Coordenação de Aperfeiçoamento de Pessoal de Nível Superior (CAPES) (to H. V.).
[S] This article contains supplemental Tables 1–5 and Figs. S1–S5.
[1] Research member of CONICET.
[2] To whom correspondence should be addressed: Cátedra de Química de Biomoléculas, Dept. de Biología Aplicada y Alimentos, Facultad de Agronomía, Universidad de Buenos Aires, Av. San Martín 4453, 1417 Buenos Aires, Argentina. Tel.: 54-11-4524-4042; Fax: 54-11-4524-8088. E-mail: ciancia@agro.uba.ar.

in their mechanisms of action could be attributed to the diversity of structures and to the fact that one compound may have more than one target protease. These differences illustrate the importance of the knowledge of specific structural characteristics of these products and their interaction with the different proteins involved in coagulation cascade in order to understand the regulation of the coagulation process and for developing new antithrombotic therapeutic agents (9). Sulfated polysaccharides from several *Codium* species showed anticoagulant activity (10). This effect was usually attributed to potentiation of antithrombin (AT)[3] and/or heparin cofactor II (HCII). However, a proteoglycan from *Codium pugniformis* showed both direct and AT-mediated inhibition for thrombin activity (11). On the other hand, sulfated polysaccharides from other *Codium* species exhibited thrombin inhibition by an HCII-dependent pathway with higher effectiveness than that of heparin or dermatan sulfate, and this effect was more potent for sulfated arabinans than for sulfated galactans (7). The driving force for the formation of the sulfated polysaccharide-protein complex was attributed to a nonspecific polar interaction between the negatively and positively charged groups in the polysaccharide and protein, respectively. The complex would be further stabilized by short range interactions (9).

In a previous paper, we reported the characterization of an extract from *C. vermilara* with high anticoagulant activity inferred from global coagulation tests (APTT and TT) (2). We report now the isolation of an arabinan and its structural characterization as a unique highly sulfated (1→3)-β-L-arabinan, with the arabinose units in the pyranose form, as well as the analysis of its anticoagulant behavior, focusing on direct thrombin inhibition mechanism.

EXPERIMENTAL PROCEDURES

Algal Sample—Samples of *C. vermilara* were collected in San Antonio Oeste (Río Negro, Argentina). They were identified according to Ref. 12. A voucher material was deposited in the herbarium of the Bernardino Rivadavia Museum (Buenos Aires, Argentina) (collection number 40466).

Isolation of the Sulfated Arabinans—Ab1 was obtained by fractionation of the room temperature water extract of *C. vermilara* (2) with potassium chloride. The raw polysaccharides (0.5 g) were dissolved in water (250 ml, 0.25%). Solid, finely divided KCl was added to the supernatant in small portions with constant and violent mechanical agitation so that the concentration was increased by 0.005–0.05 M each time. After each addition, stirring was continued for 3–5 h to ensure equilibration of the system. The upper limit of KCl concentration was 2.0 M. The precipitate, obtained at 0.115 M (Ab1, 31% p/p of the parent extract), as well as the residual solution were dialyzed (molecular weight cut-off 3,500), concentrated, and freeze-dried. By a similar procedure, a precipitate was obtained at a 0.1 M concentration of this salt from the hot water extract of the same seaweed (2). This product was highly contaminated with amylose, so it was submitted to a treatment with α-amylase (13) and then fractionated again by the addition of KCl to give a 0.1 M concentration, obtaining arabinan Ab2 (5.1% p/p of the hot water extract). A stepwise addition of NaCl to a solution of the room temperature water extract of *C. vermilara* up to 2 M yielded no precipitate.

Chemical Analyses—The total sugar content was analyzed by the phenol-sulfuric acid method (14). Sulfate was determined turbidimetrically (15). The protein content was determined colorimetrically (16). Optical rotations (sodium D-line) were measured in a PerkinElmer Life Sciences 343 polarimeter, using 0.2–0.4% solutions of the polysaccharides in water. For GC, alditol acetates were obtained by reductive hydrolysis and acetylation of the samples (17). Number average molecular weight was estimated by the method of Park and Johnson (18).

Desulfation—The reaction was carried out by the microwave-assisted method described by Navarro *et al.* (19). Ab1 (20 mg) was converted to the pyridinium salt and dissolved in 10 ml of DMSO containing 2% pyridine. The mixture was heated for 10-s intervals and cooled to 50 °C (6 times). It was dialyzed for 1 week against tap water and then for 2 days against distilled water (molecular weight cut-off 3,500) and lyophilized (yield 69%, considering the sulfate loss). An aliquot was methylated as described bellow without previous isolation of the product.

Methylation Analysis—The polysaccharide (5–10 mg) was converted into the corresponding triethylammonium salt (17) and methylated according to Ciucanu and Kerek (20); finely powdered NaOH was used as a base. The methylated derivative was hydrolyzed, and the partially methylated sugars were derivatized to the alditol acetates (17).

Gas Chromatography—GC of the alditol acetates was carried out on a Hewlett Packard 5890A gas-liquid chromatograph (Avondale, PA) equipped with a flame ionization detector and fitted with a fused silica column (0.25-mm inner diameter × 30 m) wall-coated open-tubular-coated with a 0.20-μm film of SP-2330 (Supelco, Bellefonte, PA). Chromatography was performed from 200 to 230 °C at 1 °C min^{-1}, followed by a 30-min hold for alditol acetates. For the partially methylated alditol acetates, the initial temperature was 160 °C, which was increased at 1 °C min^{-1} to 210 °C and then at 2 °C min^{-1} to 230 °C. N_2 was used as the carrier gas at a flow rate of 1 ml min^{-1}, and the split ratio was 80:1. The injector and detector temperature was 240 °C.

GC-MS-GC—MS of the methylated alditol acetates was performed on a Shimadzu GC-17A gas-liquid chromatograph equipped with a SP-2330 column interfaced to a GCMSQP 5050A mass spectrometer (Kyoto, Japan) working at 70 eV. The total helium flow rate was 7 ml min^{-1}, the injector temperature was 240 °C. Mass spectra were recorded over a mass range of 30–500 atomic mass units.

FTIR Spectroscopy—Fourier transform infrared spectra were recorded from 4,000 to 250 cm^{-1} with a 510P Nicolet FTIR spectrophotometer (Madison, WI), using dry samples in KBr. 32 scans were taken with a resolution of 4 cm^{-1}. Data collection and processing were performed on the OMNIC 7.2 (Thermo-Nicolet, Madison, WI).

NMR Spectroscopy—Samples (15–20 mg) were dissolved in D_2O solutions (0.5 ml) and lyophilized. This procedure was

[3] The abbreviations used are: AT, antithrombin; HCII, heparin cofactor II; APTT, activated partial thromboplastin time; TT, thrombin time; HMQC, heteronuclear multiple quantum coherence; MD, molecular dynamics; PT, prothrombin time(s); BT, bovine thrombin; HT, human thrombin.

repeated twice. Then the samples were dissolved in D_2O, agitated for 24 h at room temperature, and centrifuged. 500-MHz ^1H NMR, proton-decoupled 125 MHz ^{13}C NMR spectra, and two-dimensional NMR experiments (HMQC and COSY) were recorded on a Bruker AM500 spectrometer (Billerica, MA) at room temperature with external reference of tetramethylsilane. Chemical shifts were referenced to internal acetone (δ_H 2.175, δ_{CH3} 31.1). Parameters for ^{13}C NMR spectra were as follows: pulse angle 51.4°, acquisition time 0.56 s, relaxation delay 0.6 s, spectral width 29.4 kHz, and scans 25,000. For ^1H NMR spectra: pulse angle 76°, acquisition time 3 s, relaxation delay 3 s, spectral width 6250 Hz, and scans 32. Two-dimensional spectra were obtained using standard Bruker software.

Fluorescence Spectroscopy—Fluorescence spectra were measured with a Jasco FP-6500 spectrofluorimeter at 20 °C in 10 mM Tris-HCl buffer, pH 7.4. Samples containing 1 μM human thrombin (HT) were titrated with a concentrated solution of polysaccharide in a 4 × 4-mm quartz cell. After incubation for 5 min, the samples were excited at 295 nm, and emission was recorded in the range 300–430 nm. Spectral slit widths were set to 1 and 5 nm, respectively. Each spectrum is the average of six scans. In each case, the blank was subtracted, and data were corrected for dilution. Binding affinity was estimated by fitting a Hill cooperative binding model to the fluorescence intensity at 335 nm ($F = F_0 + \Delta F \times [L]^n/(K_d + [L]^n)$, where F is the measured signal, F_0 is the signal in the absence of polysaccharide, ΔF is the signal change at protein saturation with polysaccharide, K_d is the dissociation constant, and n is the Hill coefficient).

Circular Dichroism Spectroscopy—Circular dichroism (CD) spectra were measured with a Jasco J-815 spectropolarimeter. All spectra were taken at 20 °C in 10 mM Tris-HCl buffer, pH 7.4. Spectra were recorded using a 1-mm path length cell in the range 190–260 nm. Each spectrum is the average of 15 scans. For these experiments, we employed 2 μM HT and/or 10 μM polysaccharide.

General Coagulation Assays—These assays were performed with a coagulometer ST4 (Diagnostica Stago, Asnières sur Seine, France). Determinations of prothrombin time (PT), activated partial thromboplastin time (APTT), and thrombin time (TT) were assayed according to established methods (21). Reagents were supplied by Diagnostica Stago except for purified bovine thrombin (Wiener, Rosario, Argentina). Normal platelet-depleted citrated plasma (900 μl) was mixed with 100 μl of each polysaccharide sample, in different concentrations, and incubated for 1 min at 37 °C. Heparin (Sigma) and dermatan sulfate (Syntex, Buenos Aires, Argentina) were used for the comparison of anticoagulant activity of the fractions. Saline solution (0.9% NaCl) was used as control. TT-like assays were also performed with purified fibrinogen (3 mg/ml) instead of plasma. All clotting assays were performed in quadruplicate. Results were expressed as ratios obtained by dividing the clotting time achieved with the anticoagulant by the time achieved with the control.

Amydolytic Assays—Amydolytic assays were performed according to the method of Colliec *et al.* (22). 50 μl of polysaccharide solution (5–100 μg/ml) in Tris-HCl buffer, pH 7.4, containing 7.5 mM EDTA and 150 mM NaCl were mixed with 75 μl of AT or HCII (200 nM) (Diagnostica Stago). After a 2-min incubation at 37 °C, 75 μl of thrombin solution (10 units/ml for bovine thrombin or an equivalent concentration for human thrombin determined by TT assay) were added, and the mixture was incubated at 37 °C for 1 min. Then 75 μl of chromogenic substrate S-2238 1.5 mM (Chromogenix, Milan, Italy) was added, and absorbance at 405 nm was measured with a Stat Fax 303 microstrip reader. It is important to note that bovine thrombin (BT) was used in AT potentiation assays, and HT was used in the case of HCII because of its specificity. Direct inhibition of thrombin activity by the polysaccharides was determined by the same assay as described above but incorporating buffer in place of AT or HCII solutions. A non-competitive partial inhibition model was fitted to inhibition data ($V'_{max} = V_{max} \times (1 + \beta[I]/K_i)/(1 + [I]/K_i)$, where V'_{max} is the measured activity, V_{max} is the activity in the absence of polysaccharide, K_i is the thrombin-polysaccharide dissociation constant, and β is the fraction of residual activity under saturation conditions.

Electrophoresis—The ability of sulfated arabinan to modify the migration pattern of thrombin was evaluated by native and denaturing polyacrylamide gel electrophoresis (SDS-PAGE). Equal volumes of purified thrombin (165 NIH units/ml) and Ab1 (250 μg/ml) were incubated for 30 s at room temperature, and the reaction was stopped by the addition of electrophoresis sample buffer, followed by heating at 100 °C for 5 min in the case of SDS-PAGE. Electrophoresis was performed in a 4–15% precast polyacrylamide gel for use with a Mini-PROTEAN Tetra cell (Bio-Rad). Proteins were stained with 0.25% Coomassie Blue R-250 in 40% methanol and 10% acetic acid, and sulfated polysaccharides were visualized with 1% (w/v) toluidine blue O (pH 6.8).

Docking—Structures of HT and BT were retained from Protein Data Bank entries 1PPB and 1TBQ, respectively (23, 24). Both disulfated ((l-Ara*p*2,4S-(1→3)-l-Ara*p*2,4S)$_4$) and non-sulfated arabinan ((l-Ara*p*-(1→3)-l-Ara*p*)$_4$) octasaccharides were constructed based on the most prevalent conformations of their composing disaccharides, obtained from solution MD simulations, as described previously (25, 26). For these calculations, the pyranosic arabinose was only considered in its most abundant form (*i.e.* that is $^4C_1$). For the docking studies, protein and carbohydrate structures were prepared with AutoDockTools version 1.5.4 for AutoDock version 4.2 (27), using AutoGrid to generate grid dimensions and parameters to cover exosites 1 and 2, each in separated runs, of both thrombin structures. The Lamarckian genetic algorithm was applied, with default parameters, except for the maximum number of generations in each run (set to 270,000) and the number of generated docked conformations, set to 1,000, after 100 docking runs. Orientations of the oligosaccharides were selected based on binding energy, abundance of orientations, and superimposition with heparin on a cluster with a 2.0 Å cut-off.

MD Simulations—Both HT and BT were simulated in four conditions: (*a*) uncomplexed, (*b*) complexed to the non-sulfated arabinan in exosite 2, (*c*) complexed to the disulfated arabinan in exosite 2, and (*d*) complexed to the disulfated arabinan in exosite 1, in a total of eight simulations. Each of these systems was solvated in triclinic boxes using periodic boundary conditions and SPC water model. The Lincs method (28) was applied

TABLE 1

Linkage analysis of pyranosic arabinans

The arabinans were permethylated and submitted to reductive hydrolysis and acetylation. The partially methylated alditol acetates were analyzed by GC-MS. Only derivatives of L-arabinose were detected. Yield of the methylated derivative after discounting the added methoxy groups is shown. The yield of methylation was as follows: Ab1, 65.2%; Ab2, 36%; DAb1, 65.6%. 2,3,4-Ara, 2,3,4-tri-*O*-methyl-L-arabinose, etc.

Monosaccharide	Structural unit	Ab1	Ab2	DAb1
2,3,4-Ara	l-Ara*p* (1→	0.7	6.2	3.3
2,4-Ara	→3) L-Ara*p* (1→	13.3	35.0	88.0
2-Ara	→3) L-Ara*p*4S (1→	25.6	29.7	4.5
4-Ara	→3) L-Ara*p*2S (1→	9.7	7.1	3.2
	→3) L-Ara*p*2,4S (1→	50.2	22.0	1.0

to constrain covalent bond lengths, allowing an integration step of 2 fs after an initial energy minimization using the steepest descents algorithm. Electrostatic interactions were calculated with the particle mesh Ewald method (29). Temperature and pressure were kept constant at 310 K and 1.0 atm by coupling proteins, oligosaccharides, ions, and solvent to external temperature (30) and pressure (31) baths with coupling constants of $\tau = 0.1$ and 0.5 ps, respectively. The dielectric constant was treated as $\epsilon = 1$. The systems were heated slowly from 50 to 310 K, in steps of 5 ps, each one increasing the reference temperature by 50 K. After this heating, all simulations were further extended to 50 ns under a constant temperature of 310 K. All simulations were performed under the GROMACS simulation suite, version 4.0.5 (32) and GROMOS96 43a1 force field (33). In the case of thrombin-arabinan complexes, before data collection, 10-ns MD simulations were employed as equilibration, with an initial 5,000 kJ mol^{-1} restraint applied to both protein and carbohydrate. This constant force was reduced by 1,000 kJ mol^{-1} at every 2 ns, allowing water molecules and counterions to settle around the complexes.

RESULTS

Structural Studies—The room temperature water extract from green seaweed *C. vermilara* (2) was stepwise fractionated with potassium chloride, producing one sharp precipitation at 0.115 M KCl (Ab1). Ab1 is a highly sulfated arabinan, which contains 97% L-arabinose and 54.1% sulfate (as SO_3K), giving a sulfate/arabinose molar ratio of 1.8:1.0, $[\alpha]_D = +167.5°$, and number average molecular mass of 180 kDa; only traces of proteins were detected. Ab1 was desulfated, giving DAb1, which still contained 5.2% sulfate and $[\alpha]_D = +50.3°$. In addition, a similar but less sulfated arabinan (43.7%, sulfate/arabinose molar ratio 1.5:1.0) was isolated from the hot water extract of the same seaweed by an equivalent procedure (Ab2).

Methylation analysis of Ab1 showed major amounts of arabinose and 2-*O*-methylarabinose, with lesser but still significant quantities of 4-*O*-methylarabinose and 2,4-di-*O*- methylarabinose, showing that 3-linked 2,4-disulfated, 2- and 4-monosulfated, and non-sulfated arabinopyranose units are present (Table 1). The same structural units are present in Ab2 but in different quantities. The percentage of arabinose units sulfated on C-4 is similar; however, it has less than half of the disulfated units, whereas the amount of non-sulfated units is important. Methylation analysis of DAb1 showed 88% 2,4-di-*O*-methylarabinose (Table 1), in agreement with the (1→3)-linkages suggested above and confirming that most of the units in the native product are 2,4-disulfated.

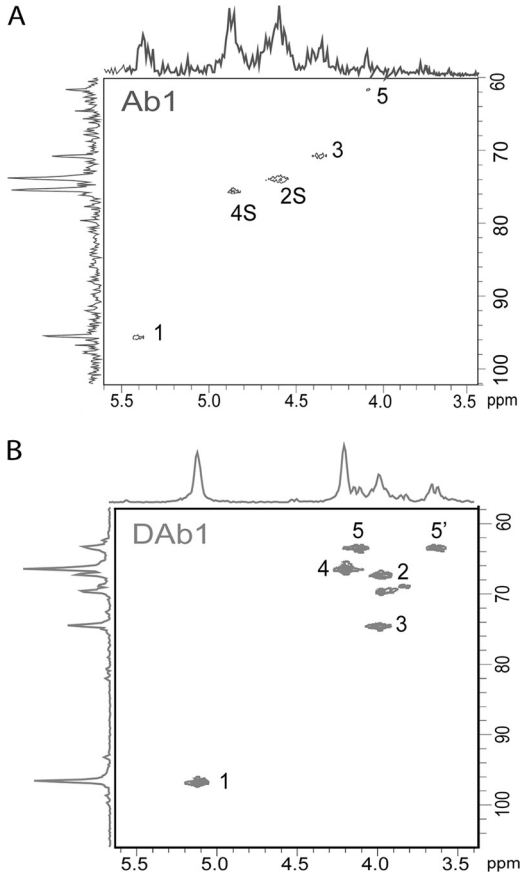

FIGURE 1. **HMQC spectra of arabinan, Ab1 (*A*), and of its desulfated derivative, DAb1 (*B*).**

The FTIR spectrum of DAb1 showed only absorptions that correspond to the carbohydrate backbone (supplemental Fig. S1). The region 855–830 cm^{-1} was previously reported as being useful to distinguish between β- and α-arabinopyranose, because the former absorbs in this range, whereas IR spectrum of the latter shows no absorptions in this zone (34). In DAb1, a small peak at 835 cm^{-1} was observed, and it was the first evidence of a β-configuration of the arabinopyranose units. Sulfate groups also give peaks in this region, and absorptions at 855 and 825 cm^{-1} in Ab1 were assigned to stretching of C4-O-S (axial) and C2-O-S (equatorial), respectively (35). In DAb1, no peaks were found at $\nu \sim 1226-1275$ cm^{-1} corresponding to the O = S = O asymmetric stretching vibration, whereas there is a strong signal in this region in the spectrum of Ab1, in agreement with previous chemical analysis.

HMQC spectra of Ab1 and DAb1 are shown in Fig. 1. Only five major carbon signals were detected in the spectrum of Ab1 (Table 2 and Fig. 1*A*). The β-L-configuration of the anomeric carbon was confirmed from the signal at 97.0 ppm in the spectrum of DAb1. The displacement of the anomeric signal in 1.5 ppm to higher fields in the spectrum of Ab1 is in agreement with the well known effect of the sulfate group at C-2 (36, 37). Similar results were found for a 2-sulfated α-L-galactan (38) and a 2-sulfated α-l-fucan (39), in which the configuration is similar to that of this arabinan (supplemental Fig. S2). Moreover,

TABLE 2

Assignment of NMR spectra of the arabinan Ab1 and its desulfated derivative, DAb1

Assignment was carried out by analysis of two-dimensional spectra and by comparison of the signals with those of related compounds. Assignment was with reference to acetone, δ_{CH3} 2.175, 31.2, used as internal standard.

	Chemical shift				
Arabinan	H1/C1	H2/C2	H3/C3	H4/C4	H5,H5′/C5
			ppm		
DAb1	5.12/97.0	3.96/67.6	3.98/74.8	4.19/66.7	4.09,3.63/63.7
Ab1	5.37/95.5	4.59/78.8	4.36/70.8	4.87/75.4	4.07/61.6

experimental and *ab initio* calculated $J_{H,H}$ coupling constants for H1-H2 and H2-H3 for galactans and fucans, which have similar configuration, confirmed a preferred $^4C_1$ conformation for the arabinose pyranose ring (40). In addition, the signal at 61.6 ppm, which corresponds to C-5 of these units (41), confirms this assignment, taking into consideration that an axial sulfate group on C-4 produces a small displacement to higher fields of the C-5 carbon signal (36). The displacement of C-2 and C-4 are those expected for substitution with sulfate groups, and the displacement of C-3 is that expected from the influence of the glycosidic linkage. Minor peaks could correspond to non-sulfated units.

The spectrum of DAb1 also shows five major carbon peaks (Fig. 1*B*) assigned to 3-linked β-L-arabinopyranose units, considering the values reported for the signals of methyl β-D-(β-L) and α-D-(α-L) arabinopyranosides (41, 42), of 3-*O*-L-arabinopyranosyl-L-arabinose (43), of the non-reducing (1→3)-β-L-arabinopyranose unit from an oligosaccharide (44), and of the effects of glycosylation in disaccharides with pyranose aglycone having the equatorial proton at one of the β-carbons (45).

Both anomeric signals in the ^{1}H NMR spectra of Ab1 and DAb1 (5.37 ppm, doublet, J = 1.5–2.5 Hz, unresolved and 5.12 ppm, doublet J = 2.3 Hz, respectively) are in agreement with a β-L-arabinopyranosidic unit in a $^4C_1$ chair conformation; the displacement to lower fields of the anomeric proton of Ab1 with respect to that of DAb1 is in agreement with sulfation on C-2.

Spectra of Ab2 show the same major peaks as those of Ab1, plus two signals at 4.03/69.5 and 4.57/73.7 ppm, which were tentatively assigned to H-2/C-2 and H-3/C-3, respectively, of 3-linked arabinopyranose units sulfated only on C-4. These results confirmed that Ab1 is constituted by major amounts of 3-linked β-L-arabinopyranose disulfated units. In DAb1, these units are mostly non-sulfated, whereas in Ab2, there are important quantities of disulfated units but also monosulfated on C-4.

Anticoagulant Activity of the Arabinans—Global clotting assays were performed on plasma incubated with Ab1, heparin, or dermatan sulfate, respectively. No clotting inhibition was observed in PT with these samples at low concentrations. However, when the concentration of the polysaccharide was increased, longer PT were observed (supplemental Table 1). These results were attributed to the presence of Polybrene in the commercial reagent (46). On the other hand, APTT and TT were prolonged in a concentration-dependent manner, and the anticoagulant activity proved to be lower than that of heparin and somewhat higher than that of dermatan sulfate (supplemental Table 1). In addition, Ab1 was compared with Ab2 and DAb1 (supplemental Table 2). The anticoagulant effect of these arabinans, which have the same backbone, was shown to be determined, as expected, by the degree of sulfation, Ab1 being the most active arabinan. In addition, coagulation time was determined with Ab1 and HT or BT, using the same conditions and reagents of the TT assay but with purified fibrinogen instead of plasma (supplemental Table 3). A significant prolongation of TT was observed for both thrombins in these conditions, although this effect was more important for BT.

In addition, there was a decrease in amydolytic activity of thrombin in the presence of increasing concentrations of Ab1. With HT and BT of equal coagulant activity determined by TT, BT showed a greater decrease in its amydolytic activity (Fig. 2*A*) (*i.e.* Ab1 exerted a higher inhibition effect on BT). A partial non-competitive inhibition model was fitted to inhibition curves. This procedure rendered a thrombin-Ab1 inhibition constant of 62 and 19 μM for HT and BT, respectively. The residual activity extrapolated at saturating concentration of Ab1 was 57% for HT and 32% for BT.

In order to establish comparisons, not in terms of concentration but in terms of effect, the APTT value obtained for a concentration of 5 μg/ml Ab1 (2.5–3 times the coagulation time of the control) was set up as the starting point. Then "equivalent" concentrations of heparin and dermatan sulfate that prolonged APTT in a similar way were determined. These concentrations of Ab1, heparin, and dermatan sulfate (5.0, 0.65, and 9 μg/ml, respectively) were used in amydolytic assays (supplemental Table 4). As expected, no direct inhibition of thrombin was observed with heparin and dermatan sulfate.

Interaction between human thrombin and Ab1 was assessed by native and SDS-PAGE (Fig. 3). When purified HT (~38 kDa) was incubated with Ab1, no changes were observed in its migration pattern in SDS-PAGE (Fig. 3*A*) because a unique protein band was visualized with Coomassie Blue. In addition, a high molecular mass band (~180 kDa) corresponding to Ab1 was visualized by staining with toluidine blue O. On the other hand, when native PAGE was performed on HT incubated with Ab1 (Fig. 3*B*), a cathodic shift with regard to the bands corresponding to Ab1 and HT was detected with both toluidine blue O and Coomassie Blue staining, suggesting the formation of a stable complex HT-Ab1.

When physiological inhibitor (AT or HCII) was added to the system, Ab1 induced an inhibition even greater on thrombin amydolytic activity. In both cases, the polysaccharide potentiated the inhibitor effect on thrombin in a concentration-dependent way (Fig. 2*B*). Compared with direct thrombin inhibition assays, there was an additional loss in residual thrombin activity. Thus, at a concentration of 5 μg/ml Ab1, the decrease in residual thrombin activity was ~50% (from 54.3 ± 5.3 to 24.1 ± 0.9% for AT and BT and from 84.2 ± 3.6 to 43.5 ± 5.9% for HCII and HT). On the other hand, in the same experimental conditions, the decrease in residual thrombin activity for heparin at the equivalent concentration (0.65 μg/ml) was ~73% for AT and ~60% for HCII.

Biophysical Characterization of Ab1-Thrombin Complex—Binding of Ab1 to HT was studied by fluorescence spectroscopy (Fig. 4*A*). Mature HT displays 9 Trp residues placed at different environments. For this reason, the emission spectrum of HT

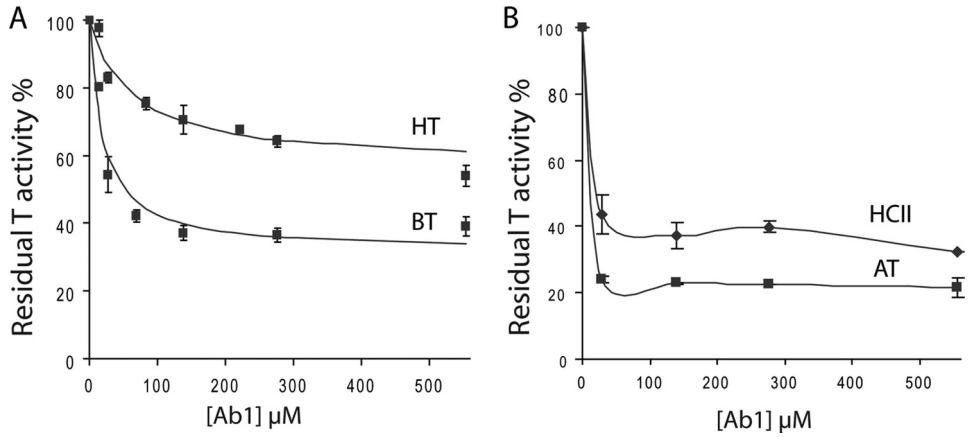

FIGURE 2. **Anticoagulant activity of Ab1.** *A*, direct inhibition of thrombin. Ab1 inhibits thrombin (BT and HB) activity, even when AT and HCII are not present. Curves obtained from a partial non-competitive inhibition model fitted best to the inhibition data. *B*, inhibition of BT activity mediated by AT and by HCII for increasing concentrations of Ab1. *Error bars*, S.E.

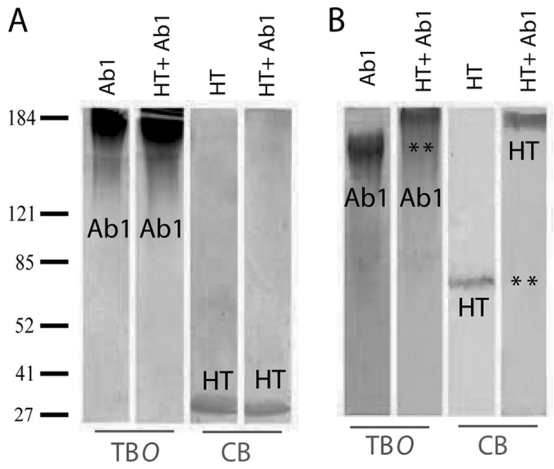

FIGURE 3. **Gel electrophoresis of Ab1 and HT and formation of a complex.** *A*, SDS-PAGE of Ab1 and HT. *B*, native electrophoresis of Ab1 and HT, in conditions similar to those used in *A*. **, absence of either HT or Ab1. *TBO*, toluidine blue O; *CB*, Coomassie Blue.

showed a broad band with a maximum at 335 nm. The addition of Ab1 induced a 2-nm red shift of the emission maximum and an increment of about 20% of the fluorescence intensity (Fig. 4*A*). A cooperative binding model described by the Hill equation was fitted to the fluorescence intensity at 345 nm (Fig. 4*B*), yielding a K_d of 17 ± 3 μM with a cooperative coefficient n of 2.1 ± 0.2.

Structural changes upon complex formation were explored by circular dichroism in the far UV. The spectrum of HT displayed features of α-helix and β-sheet (Fig. 4*C*). Deconvolution of this spectrum with the program CDSSTR using the basis SP37 rendered a content of 16.5% α-helix and 31% β-sheet. These values are in close agreement with those calculated from the Protein Data Bank file 1PPB of HT (15% α-helix and 36% β-sheet). Polysaccharide addition induced a small change in the CD spectrum of thrombin. Interestingly, the spectrum of the complex cannot be completely described as the addition of spectra of the isolated components, suggesting that either HT or Ab1 or both suffered a conformational change upon binding.

Modeling Ab1-Thrombin Interactions by MD Simulation—Considering that the conformational preferences of carbohydrates may be accessed through their composing glycosidic linkage geometries, the disaccharide units within the arabinan structures were conformationally evaluated by relaxed contour plots, followed by a solution MD refinement (supplemental Fig. S3). From these data, it was observed that the non-sulfated disaccharide showed an additional minimum energy region when compared with its sulfated counterpart. On the other hand, in solution, both glycosidic linkages showed a similar major conformational state, centered at $\phi = 90°$ and $\psi = -120°$. Based on this geometry, the octasaccharide fragments for those arabinans were built and employed as ligands during the docking procedures. Accordingly, the orientations obtained for the disulfated and non-sulfated arabinan octasaccharides on the surface of both BT and HT enclosed thrombin exosite 2, mostly superimposing heparin arrangement on the surface of thrombin, as observed in previous crystal structures (47). Additionally, because sulfated compounds have also been described to bind exosite 1 (48), docking procedures of the disulfated oligosaccharides were also carried out at such a region. Such complexes were further refined through MD simulations, from which data on the dynamics of thrombin-arabinan complexes were retrieved.

Accordingly, the binding of the disulfated arabinan oligosaccharide to exosite 2 of HT and BT affects the flexibility of several portions in the protein structure (Fig. 5, *A* and *B*). Among these regions, those around residues 60 and 77, located in close vicinity to the thrombin active site, comprise loops whose plasticity is increased in the presence of the oligosaccharide. Additionally, considering that heparin binding to exosite 2 had been shown to influence the conformation of the thrombin active site (49), such a possibility was also evaluated for the disulfated arabinan, in which the distance between atoms His-57 ND1 and Asp-102 OD1, from the catalytic triad, was observed to increase in the presence of the disulfated oligosaccharide (Fig. 5, *C* and *D*) in a disrupted conformational state (Fig. 5, *E* and *F*). Such a profile, although indicating a disturbance of the catalytic site organization, is in agreement with Ab1 anticoagulant activity, stronger over BT when compared with HT (Fig. 2*A*).

The interaction between arabinan oligosaccharides and BT or HT indicates that most protein-carbohydrate contacts

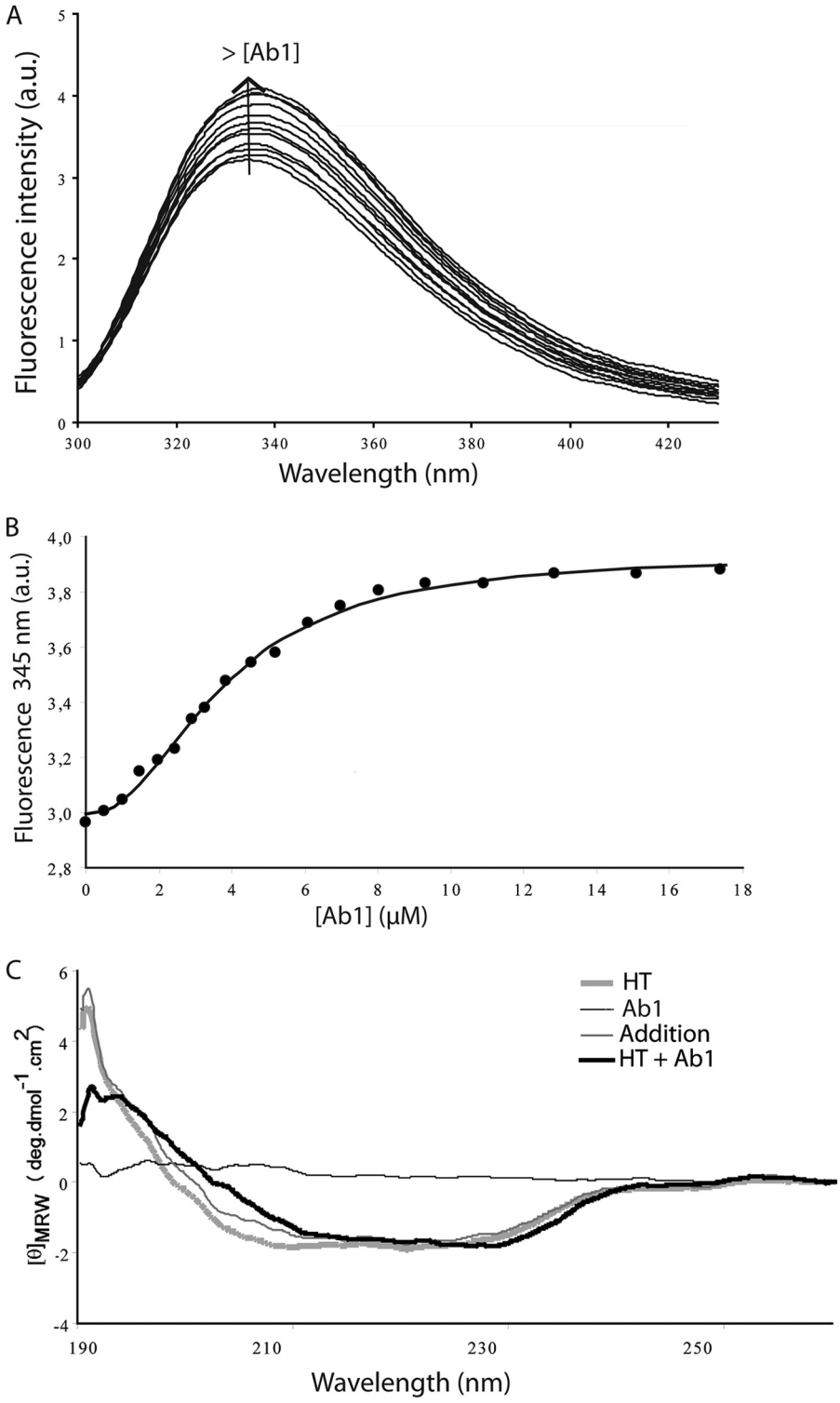

FIGURE 4. **Biophysical characterization of Ab1-HT interaction.** *A*, fluorescence spectra of HT at increasing concentration of Ab1. *B*, fluorescence intensity measured at 345 nm at increasing concentration of Ab1. *C*, far UV CD spectra of HT, Ab1, and a mixture of HT and Ab1. The addition of the spectra measured for both isolated components is also shown.

through sulfate groups are mediated by basic amino acid residues in the enzyme surface (Table 3), more than 60% of them being performed by the exosite 2-composing residues, as identified in previous mutagenesis studies (50), and more intense for BT (Table 3), whereas the remaining contacts are mostly performed by other positively charged amino acid residues. The main interaction differences between both thrombins and Ab1 may originate from the C-terminal region of the enzymes, where three variant residues may be observed (HT *versus* BT): 1) Gln-244 *versus* Arg-244, which provides an additional basic amino acid residue for interaction with Ab1 in BT; 2) Phe-245 *versus* Leu-245, which removes a bulky residue, which may

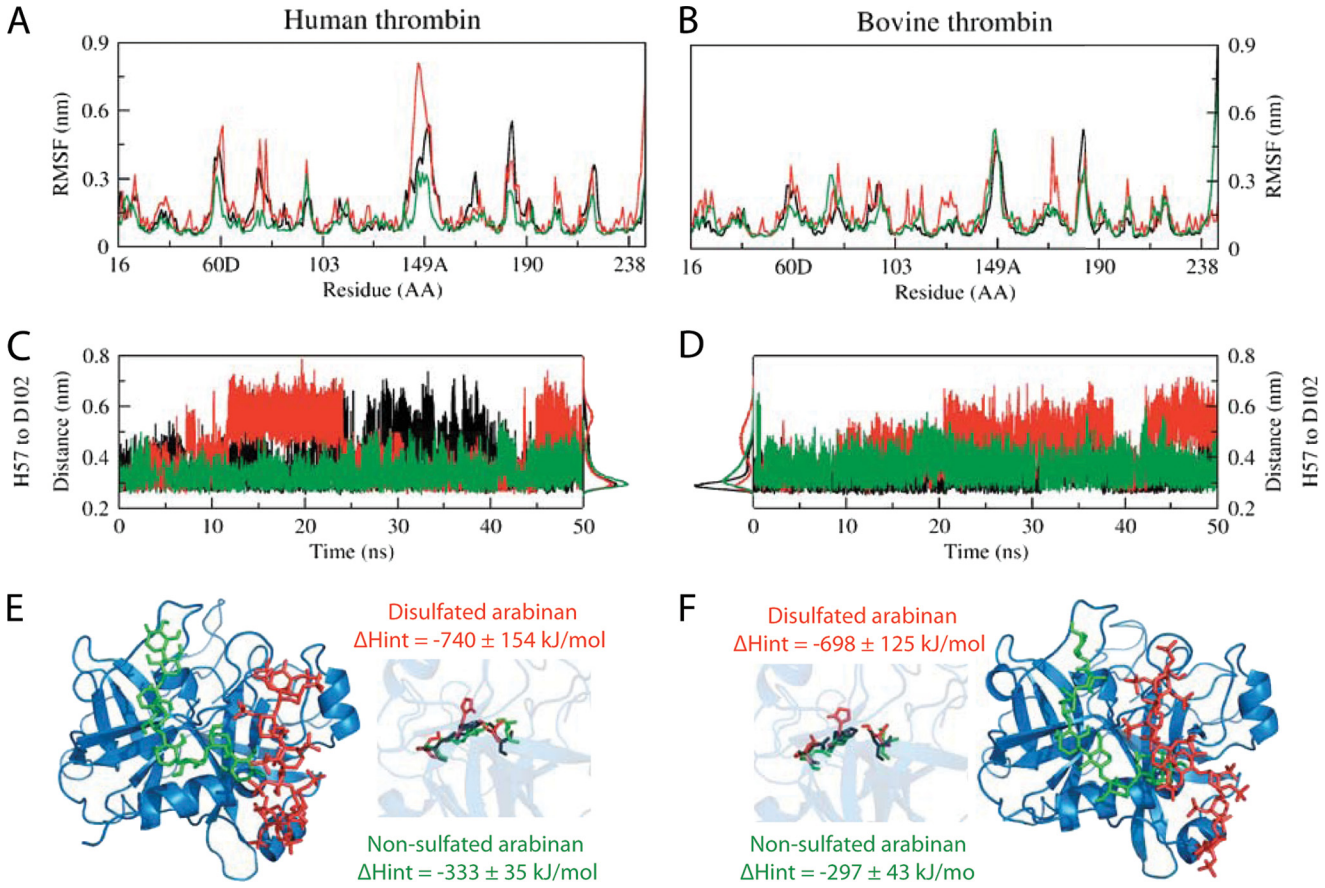

FIGURE 5. **HT and BT profiles during MD simulations in their uncomplexed (*black*), persulfated arabinan octasaccharide-complexed at exosite 2 (*red*), and non-sulfated arabinan octasaccharide-complexed at exosite 2 (*green*) states.** *A* and *B*, the root mean square fluctuation (*RMSF*) for the thrombin heavy chains are presented. In *C* and *D*, the distances between the ND1 atom of His-57 and the OD1 atom of Asp-102, which compose the thrombin catalytic triad, are presented. In *E* and *F*, the final arrangements of both studied octasaccharides, in relation to thrombin heavy chain, are shown (the protein light chain was omitted for clarity), together with the final state for the thrombin catalytic triad and the enthalpic contribution for the interaction between the complete protein and carbohydrate chains.

TABLE 3

Enthalpic contribution for the interaction between the amino acid residues of both HT and BT to disulfated and non-sulfated arabinan oligosaccharide

Calculations were carried out by MD experiments.

	Enthalpic contribution for interaction			
	(L-Ara*p*2,4S-(1→3)-L-Ara*p*2,4S)$_4$		(L-Ara*p*-(1→3)-L-Ara*p*)$_4$	
Amino acid residues (HT/BT)	HT	BT	HT	BT
	kJ/mol		*kJ/mol*	
His-91/His-91	−2 ± 2	−5 ± 9	−24 ± 7	−9 ± 6
Arg-93/Arg-93	−133 ± 29	−101 ± 45	−12 ± 7	−2 ± 3
Arg-97/Lys-97	−30 ± 41	0	0	0
Arg-101/Arg-101	−93 ± 27	−51 ± 29	−7 ± 6	−3 ± 5
Arg-126/Lys-126	−98 ± 30	−94 ± 46	0	0
Arg-165/Arg-165	−39 ± 33	0	0	0
Arg-233/Arg-233	−48 ± 34	−46 ± 33	−6 ± 5	−4 ± 8
Lys-235/Lys-235	−58 ± 29	−3 ± 5	−2 ± 2	−1 ± 1
Lys-236/Lys-236	−91 ± 38	−136 ± 43	−20 ± 12	−6 ± 8
Arg-240/Lys-240	−17 ± 25	−125 ± 53	−20 ± 5	−18 ± 8
Gln-244/Arg-244	0	−90 ± 61	−14 ± 8	−7 ± 11
Subtotal	−570 ± 99	−650 ± 117	−104 ± 18	−49 ± 20
Total	−740 ± 154	−698 ± 125	−333 ± 35	−297 ± 43

facilitate accommodation of Ab1 in the surface of BT; 3) Glu-247 *versus* Ser-247, which exchanges an acidic amino acid residue, incapable of interacting with Ab1 sulfate groups, for a polar one, which can contribute in this process donating a hydrogen bond. Additionally, in Ab1-thrombin complexes, the 2-linked sulfate groups were shown to interact more intensely with both thrombin structures than the 4-linked groups (supplemental Table 5). On the other hand, the non-sulfated arabinan octasaccharide has such interactions weakened or eliminated, although the interactions with exosite 2-composing residues were retained (Table 3). Also, the sulfate absence on such octasaccharide leads to changes of the non-sulfated arabi-

nan orientation in relation to thrombin structure, when compared with the disulfated oligosaccharide (Fig. 5, *E* and *F*).

In contrast, HT shows reduced global flexibility as due to the binding of disulfated arabinan oligosaccharide to exosite 1, whereas only point differences may be observed for BT when compared with the uncomplexed enzymes. Such a profile is maintained in the catalytic triad organization of both proteins, as evaluated for the distance between the His-57 ND1 atom and the Asp-102 OD1 atom. In other words, although complexation of the disulfated arabinan oligosaccharide to thrombin exosite 2 appears to be able to promote a conformational modification at the enzyme catalytic site, its complexation to exosite 1 does not promote major modifications in the enzyme dynamics (supplemental Fig. S4).

DISCUSSION

The system of polysaccharides synthesized by green seaweed *C. vermilara* is constituted by major amounts of sulfated L-arabinans and sulfated D-galactans. Sulfated D-galactans in green seaweeds have been previously found in other species of *Codium*, and their structures were determined (4–6, 51). Recently, a small amount of a sulfated mannan was also reported (52).

L-Arabinose is a constituent of many different cell wall components, including pectins, glucuronoarabinoxylans, arabinogalactan proteins, and extensins (53, 54). Although the pyranose form of L-arabinose is thermodynamically more stable, in these polymers, it occurs mostly in the furanose form. Terminal L-arabinopyranose has been reported on short branches of β-(1→6)-galactan of arabinogalactan proteins from different sources (55); some of the L-arabinopyranose units of wheat flour arabinogalactan protein were terminal, whereas other L-arabinopyranoses are substituted with L-arabinofuranose residues (56), but no longer sequence of L-arabinopyranose units has been found. Moreover, to the best of our knowledge, *Codium* species are the only known natural source of polymers constituted only by arabinopyranosic units. Based on these structural features, Ab1 represents a unique arabinan reported for the first time.

Sulfated arabinans were obtained from several species of *Codium* (molar ratios of sulfate/arabinose, 0.5–0.8), and their anticoagulant behavior was analyzed, but no structural details were determined (7). Two similar sulfated L-arabinans were isolated from *Codium dwarkense* (8) and *Codium latum* (57) by precipitation with 0.12 and 0.2 M KCl, respectively, and they were characterized as furanosic sulfated α-L-arabinans, the latter with (1→5)-linkages, without specification of the position of the sulfate groups. On the other hand, partial acid hydrolysis of the water extract of *C. fragile* yielded 3-*O*-β-L-arabinopyranosyl-L-arabinose (1), and the arabinans deduced from structural analysis of the room temperature water extracts from *C. fragile* and *C. vermilara* and some of the fractions obtained from them showed a linear backbone of 3-linked β-L-arabinopyranose units with major sulfate substitutions at C-2 and C-4 and a minor substitution at C-4 (2, 3).

In this work, Ab1 was isolated from the room temperature water extract of *C. vermilara* in an important yield through a sharp gelification at 0.115 M KCl. No precipitation occurred when using sodium chloride, indicating that the insolubilization is K^+-specific as in the case of κ-carrageenans. Lower or higher concentrations of potassium chloride (upper limit 2 M) did not show any other precipitation. This product is a linear 3-linked β-L-arabinopyran with major sulfation on both C-2 and C-4 and minor quantities of monosulfated units on C-4 or on C-2. The mechanism of gel formation in dilute potassium chloride solutions has been extensively studied for κ-carrageenan, where junction zones in gels are formed by quaternary interactions at the superhelical level (58) between ordered tertiary structures (double helices), promoted by potassium ions, through the one-stage domain mechanism of aggregation (coil → double helix → gel) (59). It seems likely that a similar mechanism could explain gel formation of other polysaccharides in which the primary mode of interchain association is through multistranded helices (59, 60). Ab2, less sulfated than Ab1, also precipitated with potassium chloride but at a higher concentration (0.5 M).

Thrombosis is one of the principal causes of morbidity and mortality in the world, and heparin is one of the most commonly used drugs in antithrombotic therapy (61). Because heparin can induce several side effects, such as thrombocytopenia, arterial embolism, bleeding complications, and others derived from its animal origin, like prion-related diseases (62), development of new anticoagulant drugs, and particularly direct thrombin inhibitors, is desirable (63).

Ab1 significantly increased APTT and TT in a concentration-dependent way with respect to the control. Prolongation of the APTT suggests inhibition of the intrinsic and/or common pathway of coagulation; meanwhile, the strongly extended TT indicates either thrombin inhibition (direct or mediated by AT/HCII) or impaired fibrin polymerization. A TT-like assay was performed using purified fibrinogen instead of plasma. In this case, prolongation of the coagulation time was also observed, and this was the first signal of a possible direct inhibition of Ab1 on thrombin activity, taking into account the fact that AT and HCII were absent in the test. Amydolytic assays in the absence of physiological inhibitors of thrombin confirmed our preliminary finding because an important decrease in residual thrombin activity was obtained with Ab1. Direct inhibition of thrombin by Ab1 was experimentally determined with both HT and BT, and the effect was significantly higher in the latter case. These results are in agreement with MD simulation analysis, because Ab1 proved to induce a greater alteration in the catalytic triad of BT than in the case of HT. This alteration in the geometry of the active site of thrombin could be related to the diminished activity of the enzyme on fibrinogen and chromogenic substrate observed in our results. Despite the higher inhibition of BT by Ab1, interaction of HT and Ab1 was studied in more detail due to its possible interest for human health.

Native polyacrylamide gel electrophoresis showed that Ab1 forms a stable complex with HT in the experimental conditions used because the top band that appeared when both molecules were incubated together contained protein and polysaccharide. In contrast, this complex was not observed in SDS-PAGE. These results confirm that, although interactions between Ab1 and HT are strong enough to stabilize the complex for its observation in native PAGE, no covalent interactions are established between these molecules. In addition, Ab1 binding to HT was measured by changes of their intrinsic fluorescence spectrum. Ligand addition

induced a red shift and an increment of HT emission, from which a K_d of 17 ± 3 μM can be calculated by using a cooperative binding model. The reasons underlying this behavior are not clear. Finally, CD spectra of the Ab1 complex suggested that ligand binding induced a small conformational change on HT, although we cannot rule out the possibility that the differences observed could arise from changes on Ab1 upon binding to HT.

Ab1 also produced potentiation of physiological inhibitors of thrombin: AT and HCII. The relative importance of these effects could not be clearly established, because both direct and indirect mechanisms (AT- or HCII-mediated) of inhibition of thrombin were acting together in amydolytic assays. For both indirect mechanisms, when the physiological inhibitor was added to the assay, there was an additional loss in residual thrombin activity of ~50% compared with direct thrombin inhibition assays due to the inhibition through direct and indirect mechanisms (Figs. 2, *A* and *B*). Although AT- and HCII-mediated inhibition of thrombin is reported here, we focused on the direct inhibition mechanism. Further research is required to elucidate how these additional effects work.

Regarding the relationship between structure and function, APTT and TT assays performed on Ab1, Ab2, and DAb1 showed that less sulfated arabinans are less active. Although Ab2 is still highly sulfated, in most of the monosulfated arabinose units, sulfate ester is on C-4. Thus, its weaker activity is in agreement with this structural feature because it was shown that sulfate groups on C-2 seem to interact more intensely with the structure of exosite 2 of thrombin and in agreement with the fact, previously established, that the anticoagulant activity of polysaccharides is not merely a consequence of their sulfate content but also of the sulfation pattern (9, 64). Interaction of DAb1 with thrombin is too weak to change the activity of the enzyme. Such differences may be related both to the interaction energy intensities between the enzymes and the polysaccharides and to the different orientations of disulfated and nonsulfated arabinans in relation to thrombin. Direct thrombin inhibition was already reported for other sulfated polysaccharides from seaweeds (*e.g.* highly branched fucans from brown algae (39), ulvans from *Ulva conglobata* (65), and galactans and proteoglycans from some other *Codium* species (11, 51)). However, no details about mechanisms of action at a molecular level for direct thrombin inhibition by seaweed sulfated polysaccharides were provided before.

Available direct thrombin inhibitors block thrombin interaction with its substrates by binding either to both the active site and exosite 1 (bivalent direct thrombin inhibitors) or only to the active site (univalent direct thrombin inhibitors) (63). On the other hand, heparin interacts with exosite 2 of thrombin, but it only inhibits the enzyme by an AT-dependent mechanism; meanwhile, dermatan sulfate potentiates HCII without binding to thrombin. The unusual mechanism described in this paper for Ab1, direct thrombin inhibition by interaction with exosite 2 that alters the active site without mediation of AT, could be of interest in the context of development of antithrombotic strategies targeting thrombin.

REFERENCES

1. Love, J., and Percival, E. (1964) The polysaccharides of the green seaweed *Codium fragile*. Part II. The water-soluble sulphated polysaccharides. *J. Chem. Soc.*, 3338–3345
2. Ciancia, M., Quintana, I., Vizcargüénaga, M. I., Kasulin, L., de Dios, A., Estevez, J. M., and Cerezo, A. S. (2007) Polysaccharides from the green seaweeds *Codium fragile* and *C. vermilara* with controversial effects on hemostasis. *Int. J. Biol. Macromol.* **41**, 641–649
3. Estevez, J. M., Fernández, P. V., Kasulin, L., Dupree, P., and Ciancia, M. (2009) Chemical and *in situ* characterization of macromolecular components of the cell walls from the green seaweed *Codium fragile*. *Glycobiology* **19,** 212–228
4. Bilan, M. I., Vinogradova, E. V., Shashkov, A. S., and Usov, A. I. (2007) Structure of a highly pyruvylated galactan sulfate from the pacific green alga *Codium yezoense* (Bryopsidales, Chlorophyta). *Carbohydr. Res.* **342,** 586–596
5. Farias, E. H., Pomin, V. H., Valente, A. P., Nader, H. B., Rocha, H. A., and Mourão, P. A. (2008) A preponderantly 4-sulfated, 3-linked galactan from the green alga *Codium isthmocladum*. *Glycobiology* **18,** 250–259
6. Ohta, Y., Lee, J.-B., Hayashi, K., and Hayashi, T. (2009) Isolation of sulfated galactan from *Codium fragile* and its antiviral effect. *Biol. Pharm. Bull.* **32,** 892–898
7. Hayakawa, Y., Hayashi, T., Lee, J., Srisomporn, P., Maeda, M., Ozawa, T., and Sakuragawa, N. (2000) Inhibition of thrombin by sulfated polysaccharides isolated from green seaweeds. *Biochim. Biophys. Acta* **1543,** 86–94
8. Siddhanta, A. K., Shanmugam, M., Mody, K. H., Goswami, A. M., and Ramavat, B. K. (1999) Sulphated polysaccharides of *Codium dwarkense* Boergs. from the west coast of India. Chemical composition and blood anticoagulant activity. *Int. J. Biol. Macromol.* **26,** 151–154
9. Ciancia, M., Quintana, I., and Cerezo A. S. (2010) Overview of anticoagulant activity of sulfated polysaccharides from seaweeds in relation to their structures, focusing on those of green seaweeds. *Curr. Med. Chem.* **17,** 2503–2529
10. Jurd, K. M., Rogers, D. J., Blunden, G., and McLellan, D. S. (1995) Anticoagulant properties of sulphated polysaccharides and a proteoglycan from *Codium fragile* ssp. *atlanticum*. *J. Appl. Phycol.* **7,** 339–345
11. Matsubara, K., Matsuura, Y., Hori, K., Miyazawa, K. (2000) An anticoagulant proteoglycan from the marine green alga, *Codium pugniformis*. *J. Appl. Phycol.* **12,** 9–14
12. Boraso de Zaixso, A. L. (2004) Marine Chlorophyta of Argentina. *Hist. Nat.* **3,** 95–119
13. Knutsen, S. H., and Grasdalen, H. (1987) Characterization of water extractable polysaccharides from Norwegian *Furcellaria umbricalis* (Huds) Lamour (Gigartinales, Rhodophyceae) by IR and NMR spectroscopy. *Botanica Marina* **30,** 497–505
14. Dubois, M., Gilles, K. A., Hamilton, J. K., Rebers, P. A., and Smith, F. (1956) Colorimetric method of determination of sugars and related substances. *Anal. Chem.* **28,** 350–356
15. Dodgson, K. S., and Price, R. G. (1962) A note on the determination of the ester sulphate content of sulphated polysaccharides. *Biochem. J.* **84,** 106–110
16. Lowry, O. H., Rosenbrough, N. J., and Farr, A. L. (1951) Protein measurements with the Folin phenol reagent. *J. Biol. Chem.* **193,** 265–275
17. Stevenson, T. T., and Furneaux, R. H. (1991) Chemical methods for the analysis of sulphated galactans from red algae. *Carbohydr. Res.* **210,** 277–298
18. Park, J. T., and Johnson, M. J. (1949) A sub microdetermination of glucose. *J. Biol. Chem.* **181,** 149–151
19. Navarro, D. A., Flores, M. L., and Stortz, C. A. (2007) Microwave-assisted desulfation of sulfated polysaccharides. *Carbohydr. Polym.* **69,** 742–747
20. Ciucanu, I., and Kerek, K. (1984) A simple and rapid method for the permethylation of carbohydrates. *Carbohydr. Res.* **134,** 209–217
21. Laffan, M. A., and Bradshaw, A. E. (1995) Investigation of haemostasis, in *Practical Haematology* (Dacie, J. V., and Lewis, S. M., eds) pp. 297–315, Churchill Livingstone, New York
22. Colliec, S., Fischer, A. M., Tapon-Bretaudiere, J., Boisson, C., Durand, P., and Jozefonvicz, J. (1991) Anticoagulant properties of a fucoidan fraction.

Thromb. Res. **64,** 143–154
23. Bode, W., Mayr, I., Baumann, U., Huber, R., Stone, S. R., and Hofsteenge, J. (1989) The refined 1.9 Å crystal structure of human α-thrombin. Interaction with D-Phe-Pro-Arg chloromethylketone and significance of the Tyr-Pro-Pro-Trp insertion segment. *EMBO J.* **8,** 3467–3475
24. van de Locht, A., Lamba, D., Bauer, M., Huber, R., Friedrich, T., Kröger, B., Höffken, W., and Bode, W. (1995) Two heads are better than one. Crystal structure of the insect-derived double domain Kazal inhibitor rhodniin in complex with thrombin. *EMBO J.* **14**, 5149–5157
25. Fernandes, C. L., Sachett, L. G., Pol-Fachin, L., and Verli, H. (2010) GROMOS96 43a1 performance in predicting oligosaccharide conformational ensembles within glycoproteins. *Carbohydr. Res.* **345,** 663–671
26. Pol-Fachin, L., Serrato, R. V., and Verli, H. (2010) Solution conformation and dynamics of exopolysaccharides from *Burkholderia* species. *Carbohydr. Res.* **345**, 1922–1931
27. Morris, G. M., Huey, R., Lindstrom, W., Sanner, M. F., Belew, R. K., Goodsell, D. S., and Olson, A. J. (2009) AutoDock4 and AutoDockTools4. Automated docking with selective receptor flexibility. *J. Comput. Chem.* **30,** 2785–2791
28. Hess, B., Bekker, H., Berendsen, H. J. C., and Fraaije, J. G. (1997) LINCS. A linear constraint solver for molecular simulations. *J. Comput. Chem.* **18**, 1463–1472
29. Darden, T., York, D., and Pedersen, L. (1993) Particle mesh Ewald. An N-log(N) method for Ewald sums in large systems. *J. Chem. Phys.* **98,** 10089–10092
30. Berendsen, H. J., Postma, J. P., van Gunsteren, W. F., DiNola, A., and Haak, J. R. (1984) Molecular dynamics with a coupling to an external bath. *J. Chem. Phys.* **81,** 3684–3690
31. Bussi, G., Donadio, D., and Parrinello, M. (2007) Canonical sampling through velocity rescaling. *J. Chem. Phys.* **126,** 014101
32. Hess, B., Kutzner, C., van der Spoel, D., and Lindahl, E. (2008) GROMACS 4. Algorithms for highly efficient, load-balanced, and scalable molecular simulation. *J. Chem. Theory Comput.* **4,** 435–447
33. Scott, W. R., Hünenberger, P. H., Tironi, I. G., Mark, A. E., Billeter, S. R., Fennen, J., Torda, A. E., Huber, T., Krüger, P., and van Gunsteren, W. F. (1999) The GROMOS biomolecular simulation program package. *J. Phys. Chem. A* **103,** 3596–3607
34. Spedding, H. (1962) Infrared Spectroscopy. in *Methods in Carbohydrate Chemistry. Vol. I. Analysis and Preparation of Sugars* (Whistler, R. L., and Wolfrom, M. L., eds) pp. 539–550, Academic Press, Inc., New York
35. Prado Fernandez, J., Rodríguez Vazquez, J. A., Tojo, E., and Andrade, J. M. (2003) Quantitation of λ-, ι-, and κ-carrageenan by midinfrared spectroscopy and PLS regression. *Anal. Chim. Acta* **480,** 23–37
36. Stortz, C. A., and Cerezo, A. S. (1992) The ^{13}C NMR spectroscopy of carrageenans. Calculation of chemical shifts and computer-aided structural determination. *Int. J. Biol. Macromol.* **14**, 237–242
37. Noseda, M. D., and Cerezo, A. S. (1993) Room temperature, low-field ^{13}C-n.m.r. spectra of degraded carrageenans. Part III. Autohydrolysis of a λ carrageenan and of its alkali-treated derivative. *Int. J. Biol. Macromol.* **15,** 177–181
38. Cinelli, L. P., Andrade, L., Valente, A. P., and Mourão, P. A. (2010) Sulfated α-L-galactans from the sea urchin ovary. Selective 6-desulfation as eggs are spawned. *Glycobiology* **20,** 702–709
39. Pereira, M. S., Vilela-Silva, A. C., Valente, A. P., and Mourão, P. A. (2002) A 2-sulfated, 3-linked α-L-galactan is an anticoagulant polysaccharide, *Carbohydr. Res.* **337,** 2231–2238
40. Becker, C. F., Guimarães, J. A., Mourão, P. A., and Verli, H. (2007) Conformation of sulfated galactan and sulfated fucan in aqueous solutions. Implications to their anticoagulant activities. *J. Mol. Graph. Model.* **26,** 391–399
41. Bock, K., and Pedersen, C. (1983) Carbon-13 nuclear magnetic resonance spectroscopy of monosaccharides. *Adv. Carbohydr. Chem. Biochem.* **41**, 27–66
42. Zhuo, K., Liu, H., Zhang, X., Liu, Y., and Wang, J. (2008) A ^{13}C NMR study on the interactions of calcium chloride/potassium chloride with pyranosides in D_2O. *Carbohydr. Res.* **343**, 2428–2432
43. Odonmazig, P., Ebringerová, A., Machová, E., and Alföldi, J. (1994) Structural and molecular properties of the arabinogalactan isolated from Mongolian larchwood (*Larix dahurica* L.). *Carbohydr. Res.* **252**, 317–324
44. Ishii, T., Konishi, T., Ito, Y., Ono, H., Ohnishi-Kameyama, M., and Maeda, I. (2005) A β-(1→3)-arabinopyranosyltransferase that transfers a single arabinopyranose onto arabino-oligosaccharides in mung bean (*Vigna radiate*) hypocotyls. *Phytochemistry* **66**, 2418–2425
45. Shashkov, A. S., Lipkind, G. M., Knirel, Y. A., and Kochetkov, N. K. (1988) Stereochemical factors determining the effects of glycosylation on the ^{13}C chemical shifts in carbohydrates. *Magn. Res. Chem.* **26,** 735–747
46. Carroll, W. E. (1999) Thromboplastins, heparin, and Polybrene. *Am. J. Clin. Pathol.* **111,** 565
47. Li, W., Johnson, D. J., Esmon, C. T., and Huntington, J. A. (2004) Structure of the antithrombin-thrombin-heparin ternary complex reveals the antithrombotic mechanism of heparin. *Nat. Struct. Mol. Biol.* **11,** 857–862
48. Salvagnini, C., Michaux, C., Remiche, J., Wouters, J., Charlier, P., and Marchand-Brynaert, J. (2005) Design, synthesis and evaluation of graftable thrombin inhibitors for the preparation of blood-compatible polymer materials. *Org. Biomol. Chem.* **3,** 4209–4220
49. Fredenburgh, J. C., Stafford, A. R., and Weitz, J. I. (1997) Evidence for allosteric linkage between exosites 1 and 2 of thrombin. *J. Biol. Chem.* **272,** 25493–25499
50. Sheehan, J. P., and Sadler, J. E. (1994) Molecular mapping of the heparin-binding exosite of thrombin. *Proc. Natl. Acad. Sci. U.S.A.* **91,** 5518–5522
51. Matsubara, K., Matsuura, Y., Bacic, A., Liao, M., Hori, K., and Miyazawa, K. (2001) Anticoagulant properties of a sulfated galactan preparation from a marine green alga, *Codium cylindricum*. *Int. J. Biol. Macromol.* **28,** 395–399
52. Fernández, P. V., Estevez, J. M., Cerezo, A. S., and Ciancia, M. (2012) Sulfated β-D-mannan from the green seaweed *Codium vermilara*. *Carbohydr. Polym.* **87,** 916–919
53. Sommer-Knodsen, J., Bacic, A., and Clarke, A. E. (1998) Hydroxyproline-rich plant glycoproteins. *Phytochemistry* **47,** 483–497
54. Somerville, C., Bauer, S., Brininstool, G., Facette, M., Hamann, T., Milne, J., Osborne, E., Paredez, A., Persson, S., Raab, T., Vorwerk, S., and Youngs, H. (2004) Towards a systems approach to understanding plant cell walls. *Science* **306,** 2206–2211
55. Clarke, A. E., Anderson, R. L., and Stone, B. A. (1979) Form and function of arabinogalactans and arabinogalactan-proteins. *Phytochemistry* **18,** 521–540
56. Tryfona, T., Liang, H.-C., Kotake, T., Kaneko, S., Marsh, J., Ichinose, H., Lovegrove, A., Tsumuraya, Y., Shewry, P. R., Stephens, E., and Dupree P. (2010) Carbohydrate structural analysis of wheat flour arabinogalactan protein. *Carbohydr. Res.* **345**, 2648–2656
57. Uehara, T., Takeshita, M., and Maeda, M. (1992) Studies on anticoagulant-active arabinan sulfates from the green alga, *Codium latum*. *Carbohydr. Res.* **23**, 309–311
58. Nilsson, S., and Piculell, L. (1991) Helix-coil transitions of ionic polysaccharides analyzed within the Poisson-Boltzmann cell model. 4. Effects of site-specific counterion binding. *Macromolecules* **24,** 3804–3811
59. Robinson, G., Morris, E. R., and Rees, D. A. (1980) Role of double helices in carrageenan gelation. The domain model. *J. Chem. Soc. Chem. Commun.*, 152–153
60. Aspinall G. O. (1982) Isolation and fractionation of Polysaccharides. in *The Polysaccharides.* Vol. 1 (Aspinall, G. O., ed) pp. 19–34, Academic Press, Inc., Orlando, FL
61. Kelton, J. G., and Warkentin, T. E. (2008) Heparin-induced thrombocytopenia. A historical perspective. *Blood* **112,** 2607–2616
62. Kam, P. C., Kaur, N., and Thong, C. L. (2005) Direct thrombin inhibitors. Pharmacology and clinical relevance. *Anaesthesia* **60,** 565–574
63. Di Nisio, M., Middeldorp, S., and Büller, H. R. (2005) Direct thrombin inhibitors. *N. Engl. J. Med.* **353,** 1028–1040
64. Melo, F. R., Pereira, M. S., Foguel, D., and Mourão, P. A. (2004) Antithrombin-mediated anticoagulant activity of sulfated polysaccharides. Different mechanisms for heparin and sulfated galactans. *J. Biol. Chem.* **279,** 20824–20835
65. Mao, W., Zang, X., Li, Y., and Zhang, H. (2006) Sulfated polysaccharides from marine algae *Ulva conglobata* and their anticoagulant activity. *J. Appl. Phycol.* **18,** 9–14